

## Article

# Analysis of the Effects of Different Factors on Damage Potential Ranking

Qinghui Lai <sup>1,2</sup> , Jinjun Hu <sup>3,\*</sup>, Lili Xie <sup>1,2,3</sup> and Longjun Xu <sup>1,2</sup><sup>1</sup> State Key Laboratory of Precision Blasting, Jiangnan University, Wuhan 430056, China<sup>2</sup> Hubei Key Laboratory of Blasting Engineering, Jiangnan University, Wuhan 430056, China<sup>3</sup> Key Laboratory of Earthquake Engineering and Engineering Vibration, Institute of Engineering Mechanics, China Earthquake Administration, Harbin 150080, China

\* Correspondence: hujinjun@iem.ac.cn

**Abstract:** A quantitative evaluation of the damage potential of ground motions to structures can provide a basis for the selection of input ground motions. To determine the main factors influencing the damage potential ranking of ground motions, the corresponding effect factors were analyzed. First, the structural period range from 0.05 to 10 s was divided into three types of period ranges based on an improved Newmark–Hall spectrum. The intensity measures (*IMs*) that can characterize the damage potential in every period range were determined. Second, the effect of yield strength coefficient ( $C_y$ ), vibration period ( $T$ ), and type of site on the damage potential ranking are explained. A recommended damage potential ranking is given in the same period range. Finally, to demonstrate the rationality of the recommended damage potential ranking in this paper, two representative reinforced concrete (RC) shear structure models are established for analysis. For the same type of structures, the damage potential rankings under different  $C_y$  and  $T$  conditions have high correlation with the recommended damage potential ranking, and the discreteness is very low. When considering the site factors, the corresponding correlation and dispersion change little. Based on the analysis of two typical structural models, the  $R^2$  between the recommended damage potential ranking and structural response ranking were 0.89 and 0.94, respectively. It is proven that the methods of  $C_y$ ,  $T$ , and the type of site are reasonable when establishing the recommended damage potential ranking in this paper. This study provides a theoretical basis for simplifying the evaluation of ground motion damage potential and for selecting input ground motions.



**Citation:** Lai, Q.; Hu, J.; Xie, L.; Xu, L. Analysis of the Effects of Different Factors on Damage Potential Ranking. *Sustainability* **2023**, *15*, 1583. <https://doi.org/10.3390/su15021583>

Academic Editor: Claudia Casapulla

Received: 16 November 2022

Revised: 23 December 2022

Accepted: 11 January 2023

Published: 13 January 2023



**Copyright:** © 2023 by the authors. Licensee MDPI, Basel, Switzerland. This article is an open access article distributed under the terms and conditions of the Creative Commons Attribution (CC BY) license (<https://creativecommons.org/licenses/by/4.0/>).

**Keywords:** damage potential ranking; period ranges dividing; yield strength coefficient; vibration period; type of site

## 1. Introduction

The damage potential ranking of ground motions refers to ground motions ranked according to the intensity measures (*IMs*) that can characterize the structural damage subjected to ground motions. An accurate evaluation of the damage potential of ground motions to structures is very important for selecting input ground motions in a seismic design [1–6]. When evaluating the damage potential of ground motion to structures, the effects of the seismic factor and structural parameter factor cannot be ignored. This is especially true when the *IMs* are selected to evaluate the damage potential, which includes both the characteristics of ground motion and structure. When these *IMs* change, the intensity of the damage potential obtained may also change. Structural parameters mainly include the vibration period ( $T$ ), yield strength coefficient ( $C_y$ ), post-yield stiffness ratio ( $k_2$ ), damping ratio ( $\zeta$ ), ductility demand coefficient ( $u$ ), etc. Some experts have used a response spectrum to evaluate damage potential. The latest papers [7,8] have studied the effects of different hysteretic models on constant-ductility response spectrum by using a large number of ground motion records, and this study mainly analyzed the effects of different  $T$ ,  $u$ ,  $k_2$ , and  $\zeta$  on the variation of the constant-ductility response spectrum.

Yi et al. [9] compared the advantages and disadvantages of the constant-strength ductility spectrum and constant-ductility strength demand spectrum and concluded that the calculation method of constant-strength ductility spectrum is simpler and does not require iterative calculation. Rosso et al. [10] analyzed the corrosion effects on the capacity and ductility of concrete half-joint bridges. Ji et al. [11] studied the effect of the ductility demand coefficient on the constant-ductility strength demand spectrum, and they found that, with an increase or decrease in the ductility demand coefficient, the strength demand coefficient and the seismic resistance coefficient showed a specific variation law. In addition, the effects of  $k_2$ ,  $\zeta$ , the hysteretic model, and pinching on the constant-strength ductility demand spectrum were also studied [12–15].

In addition to studying the effects of structural parameters, the studies [16–19] also analyzed the effect of seismic information factors on the constant-strength response spectrum and constant-ductility response spectrum. Seismic information mainly includes magnitude, epicenter distance, type of site, etc. Miranda et al. [18,19] explained in detail the effect of magnitude, epicenter distance, and other factors on the constant-ductility response spectrum. Lu et al. [16] studied the effects of the type of site, designed ground motion grouping, and other factors on the constant-strength ductility demand spectrum. When the yield strength coefficient is fixed, the ductility demand spectrum of the structure has great relationships with site condition, designed ground motion grouping, and other factors. It can be concluded that the structural parameters such as  $C_y$  and  $T$ , and the seismic factors such as the type of site are important factors that must be considered when studying the damage potential of the structure caused by ground motions. Many experts have also conducted studies on this.

The above studies mostly focused on the effects of these factors on the variation law of the elastic–plastic mean response spectrum or median response spectrum; however, few have studied the effects of these factors on the relative variation in damage potential parameters for many ground motions. That is, few experts have studied the effects of these factors on the damage potential ranking of ground motions. Baker [19–23] calculated the correlations of  $\varepsilon$  at different periods when he selected the input ground motions based on the conditional mean spectrum. This paper mainly focused on the effects of  $C_y$ ,  $T$ , and site factors on the damage potential ranking. Firstly, the period range from 0.05 to 10 s was divided into three period ranges based on the improved Newmark–Hall spectrum. The structures in the same period range were analyzed as the same type of structures, and a recommended damage potential ranking is given to replace all rankings under different  $C_y$  and  $T$  conditions. Then, we selected the optimal  $IM$  to evaluate the damage potential of ground motions for every type of structure rather than an individual structure and studied the effects of the relevant factors on the ranking of damage potential. Finally, two typical multi degree of freedom (MDOF), concrete-reinforced (RC) shear structure models were established to demonstrate the variation law obtained in this paper. The technical framework of this paper is shown in Figure 1.

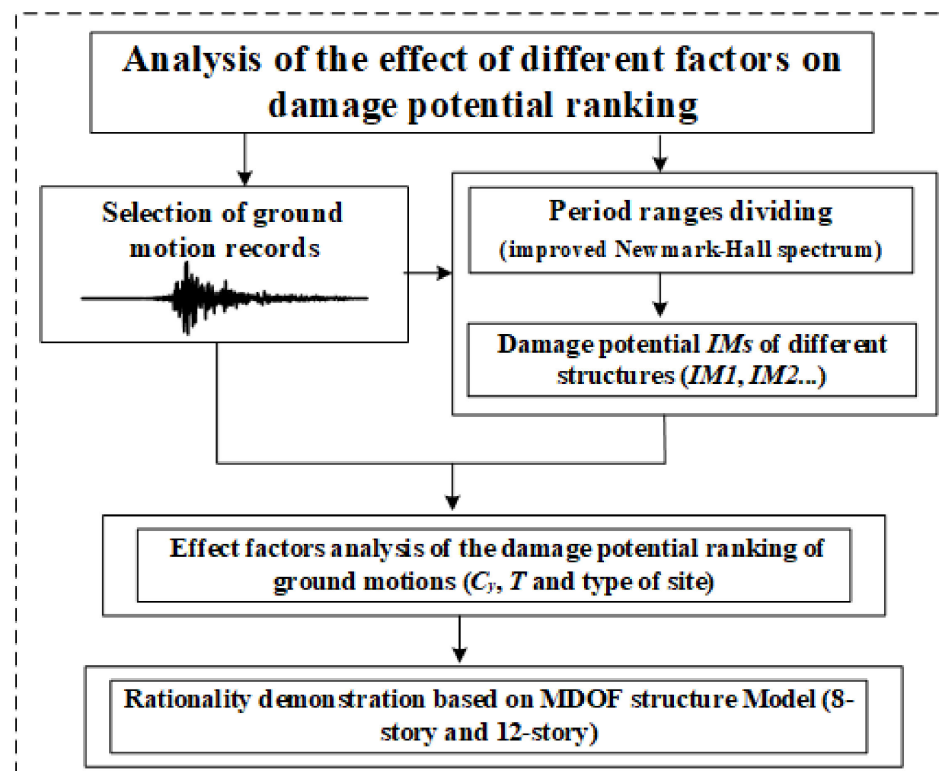


Figure 1. Technical framework of this paper.

## 2. Selection of Ground Motions

The ground motions used in this study were selected from the NGA-West2 database. When studying the effect of  $C_y$ ,  $T$ , and type of site on the damage potential ranking, the ground motion records with larger damage potential should be selected for analysis. Therefore, 5535 horizontal ground motion records with peak ground acceleration (PGA) greater than 0.05 g were selected [24]. The elastic acceleration response spectra of the selected ground motion records are shown in Figure 2. To analyze the effect of the type of site, the site classification of ground motion records is carried out based on  $V_{s30}$  information and Guo's [25] method, and the selected ground motion records are divided into four types. The classification criterion and results are shown in Table 1.

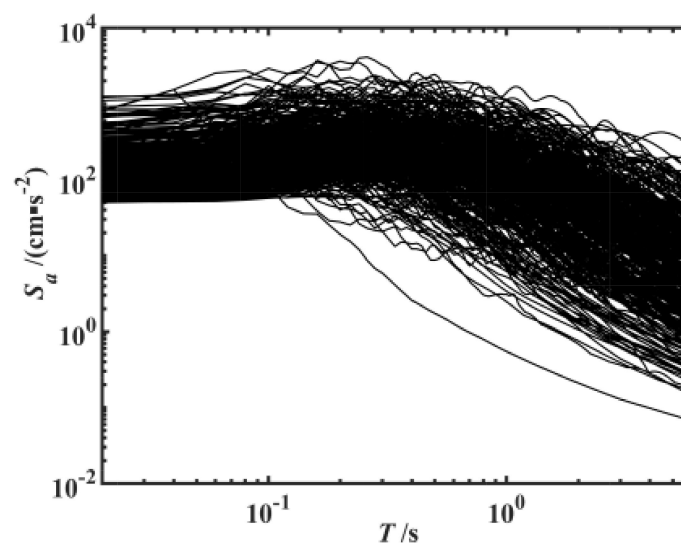


Figure 2. Acceleration response spectrum of selected ground motion records ( $\zeta = 0.05$ ).

**Table 1.** Site classification results of ground motion records based on  $V_{s30}$ .

Type of Sites	Range of $V_{s30}$ (m·s <sup>-1</sup> )	Number
Type I site	$V_{s30} > 550$	846
Type II site	$265 < V_{s30} < 550$	3646
Type III site	$165 < V_{s30} < 265$	979
Type IV site	$V_{s30} \leq 165$	64

### 3. Period Range Dividing Based on Improved Newmark–Hall Spectrum

When the *IMs* selected to evaluate the damage potential are related to the vibration period (such as  $S_a(T_1)$ ,  $S_v(T_1)$ ,  $S_d(T_1)$ , etc.), the damage potential ranking will also change when the period changes. There are countless period points within a certain period range from 0 to 10 s. When  $T$  changes within a small period range, the change in the corresponding damage potential ranking is very small. The greater the size of the period range, the more obvious the differences in the damage potential rankings. Therefore, the adjacent periods with small changes in the damage potential ranking of ground motions can be combined into a smaller period range. Additionally, in this period range, the damage potential ranking at a different period changes little, which can be expressed using the same damage potential ranking [26].

The improved Newmark–Hall spectrum has a good application in dividing the structural period range. In the early calibration of the seismic design spectrum, there are relevant applications for solving the empirical expression of a design spectrum [27,28]. This paper also uses the improved Newmark–Hall spectrum [29] to divide the period range. The interest period range from 0.05 to 10 s in this paper, and 200 periods with a period interval of 0.05 s, are selected. Additionally, this period range is divided into three small period ranges: acceleration, velocity, and displacement sensitive period ranges (short-period range, medium-period range, and long-period range). It is assumed that the variation in damage potential rankings of ground motions is very small in the same period range. Therefore, the average value of damage potential *IM* at different periods of the same period range can be selected to characterize the damage potential of ground motions for structures of the same types. The effect of  $T$  in the same structural range is analyzed later in this paper. The principle of the improved Newmark–Hall spectrum to divide the structural period is shown in Equation (1).

$$C = \sum_{T=0}^{10} (C_{NRS_A}(T_1) + C_{NRS_V}(T_2) + C_{NRS_D}(T_3)) \quad (1)$$

where  $C$  is the variation coefficient,  $NRS_A$ ,  $NRS_V$ , and  $NRS_D$  are the acceleration response spectrum, velocity response spectrum, and displacement response spectrum normalized by  $PGA$ ,  $PGV$  and  $PGD$ , respectively. There are two boundary period points:  $t_1$ ,  $t_2$ ,  $0.05 \text{ s} < T_1 < t_1$ ,  $t_1 < T_2 < t_2$ , and  $t_2 < T_3 < 10 \text{ s}$ .

The principle of dividing the period range works as follows: when the value of  $C$  is at a minimum, the boundary period point of the three period ranges can be obtained. The dividing range results of the structural period can be seen in Figure 3 and Table 2.  $NRS_C$  is the distribution of variation coefficient with  $T$  based on the improved Newmark–Hall spectrum. The dividing period range results of the short-period range, medium-period range, and long-period range are slightly different from those given in the literature [8] when selecting the most unfavorable designed ground motions.

**Table 2.** Structural period dividing results based on improved Newmark–Hall spectrum.

Short-Period Range	Medium-Period Range	Long-Period Range
$T < 0.40 \text{ s}$	$0.40 \text{ s} \leq T < 1.55 \text{ s}$	$T \geq 1.55 \text{ s}$

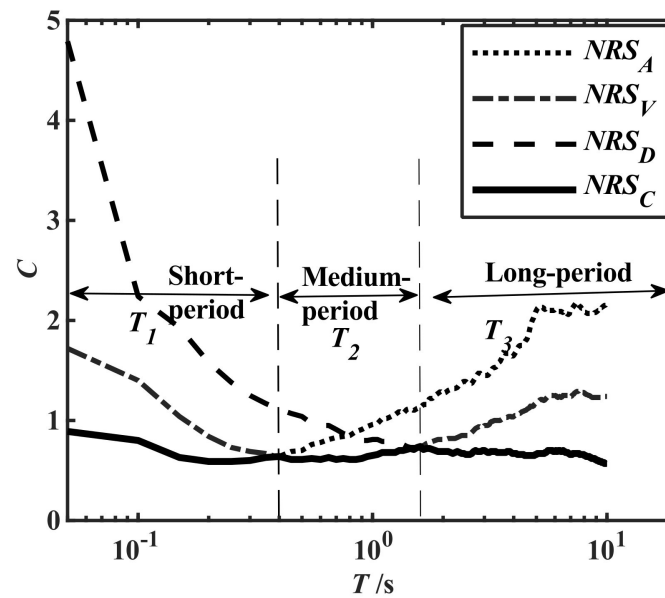


Figure 3. Structural period dividing results based on an improved Newmark–Hall spectrum.

#### 4. Selection of Damage Potential IMs and Statistical Parameters

According to the relative studies [30–34], the strength damage mainly occurs in the short-period structures subjected to the ground motions, and the acceleration response is generally selected by the engineering demand parameters (EDPs). The ductile damage mainly occurs in the medium-period and long-period structures subjected to the ground motions, and the displacement response is generally selected as the EDP. Therefore, the corresponding inelastic acceleration response spectrum mean value  $S_a(T_{ave}, C_{y,ave})$  and displacement response spectrum mean value  $S_d(T_{ave}, C_{y,ave})$  of a single degree of freedom (SDOF) are studied as the damage potential IMs of ground motions. The  $C_y$  reflects the nonlinear degree of the structures subjected to ground motions.  $S_a(T_{ave}, C_{y,ave})$  and  $S_d(T_{ave}, C_{y,ave})$  are the average values of damage potential IMs under different  $C_y$  and  $T$  conditions in the same period range. This paper also demonstrates and analyzes the rationality of the selected IMs. A bilinear model was selected as the nonlinear model, and the hysteretic skeleton curve is shown in Figure 4.  $f_y$  is the yield strength,  $K_0$  is the initial stiffness,  $k_2K_0$  is the post-yield stiffness ratio,  $u_y$  is the yield displacement, and  $u_{max}$  is the maximum displacement. To accurately evaluate the effect of  $C_y$ ,  $T$ , and the type of site on the damage potential ranking, the Spearman correlation coefficient ( $R$ ), standard deviation ( $\delta$ ), and determination coefficient ( $R^2$ ) are used in this paper to describe the correlation and discreteness of two variables [35].

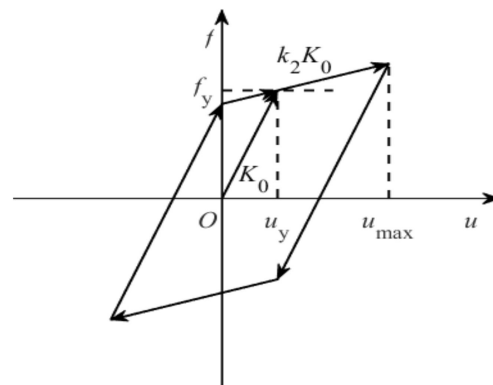


Figure 4. Bilinear hysteretic skeleton curve used in this paper.

## 5. Analysis of the Effects of Different Factors on the Damage Potential Ranking

In this paper, the recommended damage potential ranking is used to predict the structural response ranking, which refers to the relative measure of the structural response caused by different ground motions, rather than the traditional specific prediction equation for the structural response of a case. It is usually assumed that the structural response and  $IMs$  of the ground motion demand the following models in traditional methods.

$$\log_{10}(EDP) = a * \log_{10}(IM) + b \quad (2)$$

The structural response of only one structure can be predicted by using this prediction equation, and the prediction equation will change when the structure changes. However, this paper aimed to predict the response ranking of all structures in a specific period range using the recommended damage potential ranking. In this paper, the period range from 0 to 10 s is divided into three period ranges based on the Newmark–Hall spectrum. The specific practices are as follows. Firstly, a group of ground motions are ranked according to the values of damage potential and structural response to obtain two kinds of ranking results,  $R_{IM}$  and  $R_{EDP}$ . If the damage potential can fully characterize the structural response, then the following equation holds.

$$R_{IM} = R_{EDP} \quad (3)$$

This situation generally does not exist because there is little discreteness and a strong correlation between the two ranking results when the  $IM$  can better predict the structural response.

### 5.1. Effects of $C_y$ and $T$

To analyze the effect of  $C_y$  and  $T$  on the damage potential ranking, 5535 ground motion records are used for correlation analysis. The calculated  $R$  and  $\delta$  results of the recommended damage potential ranking in the short-period, medium-period, and long-period ranges and the damage potential ranking under different  $C_y$  and  $T$  conditions of the same period ranges are shown in Figure 5. The average values of  $R$  and  $\delta$  of the structures of the same types are shown in Table 3. From the results, it can be concluded that the  $R$  between the recommended damage potentials ranking and the damage potentials rankings under different  $C_y$  and  $T$  conditions of the same period range was more than 0.8, and the average value was more than 0.9; therefore, the correlation was very strong. The average  $\delta$  was about 0.2, which proves that the dispersion is very small, and the damage potential of multiple periods in the same period range can be replaced by their average values. Therefore,  $S_d(T_{ave}, C_{y,ave})$  and  $S_d(T_{ave}, C_{y,ave})$  are reasonable as the recommended damage potential  $IMs$  in the same period range.

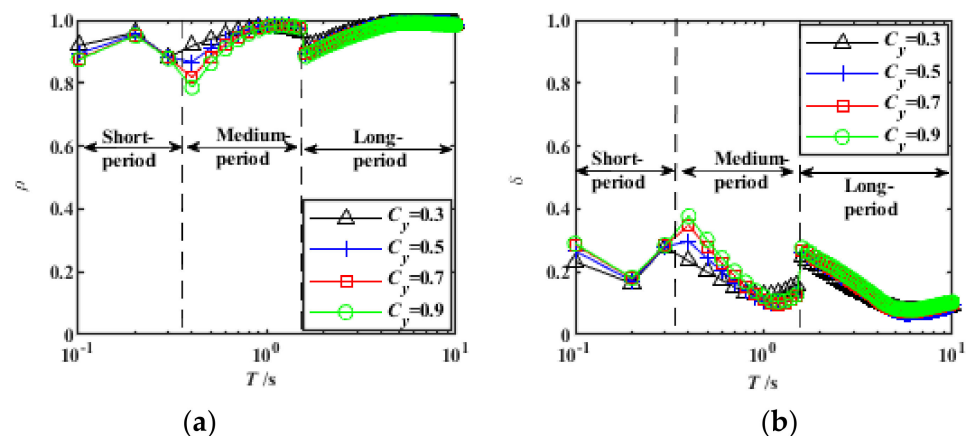


**Figure 5.** Correlation and discreteness analysis results between the recommended damage potential ranking and damage potential ranking under different  $C_y$  and  $T$  conditions: (a) correlation analysis result; (b) discreteness analysis result.

**Table 3.** Mean correlation coefficient and standard deviation between recommended damage potential ranking and damage potential ranking under different  $C_y$  and  $T$  conditions.

$C_y$	Short-Period Range		Medium-Period Range		Long-Period Range	
	R	$\delta$	R	$\delta$	R	$\delta$
$C_y = 0.3$	0.921	0.225	0.963	0.155	0.980	0.106
$C_y = 0.5$	0.911	0.239	0.960	0.152	0.979	0.110
$C_y = 0.7$	0.903	0.249	0.951	0.163	0.977	0.114
$C_y = 0.9$	0.901	0.252	0.942	0.177	0.975	0.119
Average	0.909	0.241	0.954	0.162	0.978	0.111

5.2. Effect of Type of Site

The site conditions are closely related to the characteristic period of the ground motions. When the natural vibration period of the structure is close to the characteristic period of the ground motion, the resonance effect will occur, which will strongly increase the structural response. To analyze the effect of the site category on the damage potential ranking, the discreteness and correlation analysis between the damage potential recommended ranking and the damage potential ranking under different  $C_y$  and  $T$  conditions in the same period range are calculated in each type of site, and the calculated results are shown in Figures 6 and 7. The results are compared with those that do not consider the site factor in Figure 5. The calculated  $R$  and  $\delta$  results between the recommended damage potential ranking and the damage potential ranking under different  $C_y$  and  $T$  conditions in the same period range are shown in Table 4. It can be concluded from the results that, for the same types of structures, whether site factors are considered or not, the  $R$  and  $\delta$  results showed little change. The statistical results show that the site factors have little effect on the correlation and discreteness of the recommended damage potential ranking and the ranking under different  $C_y$  and  $T$  conditions. Therefore, it is unnecessary to consider site factors when selecting recommended input ground motions based on the damage potential ranking of ground motions.

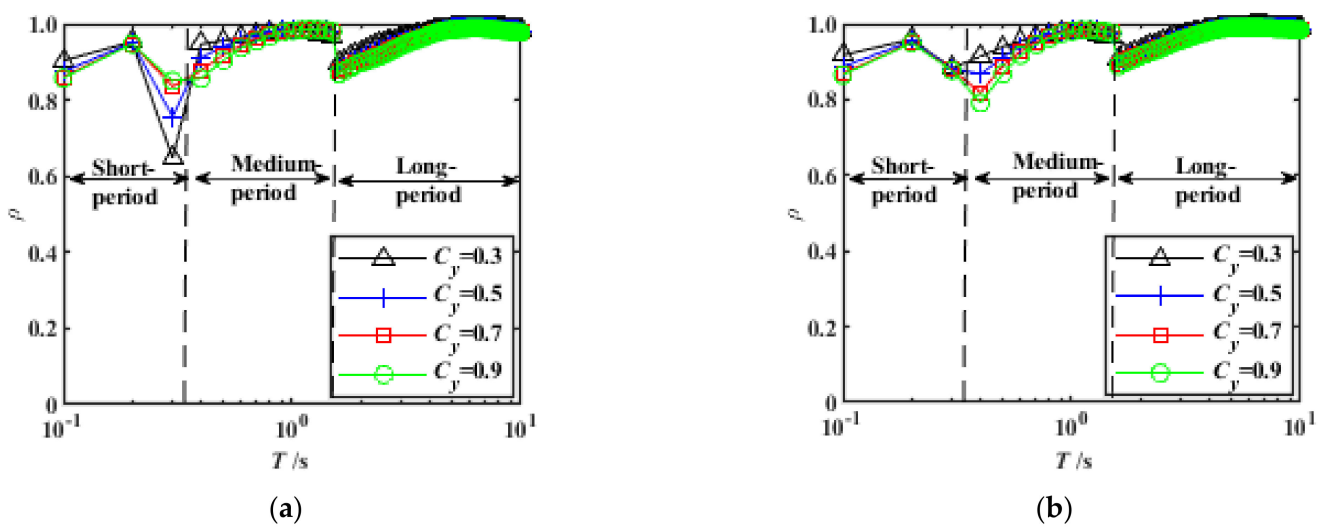
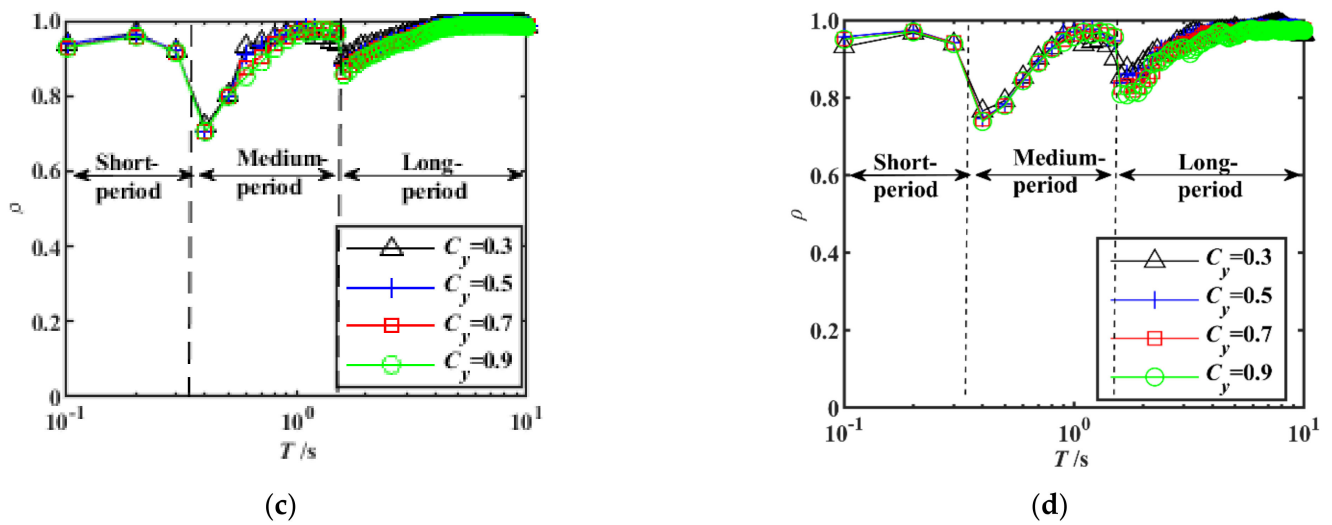
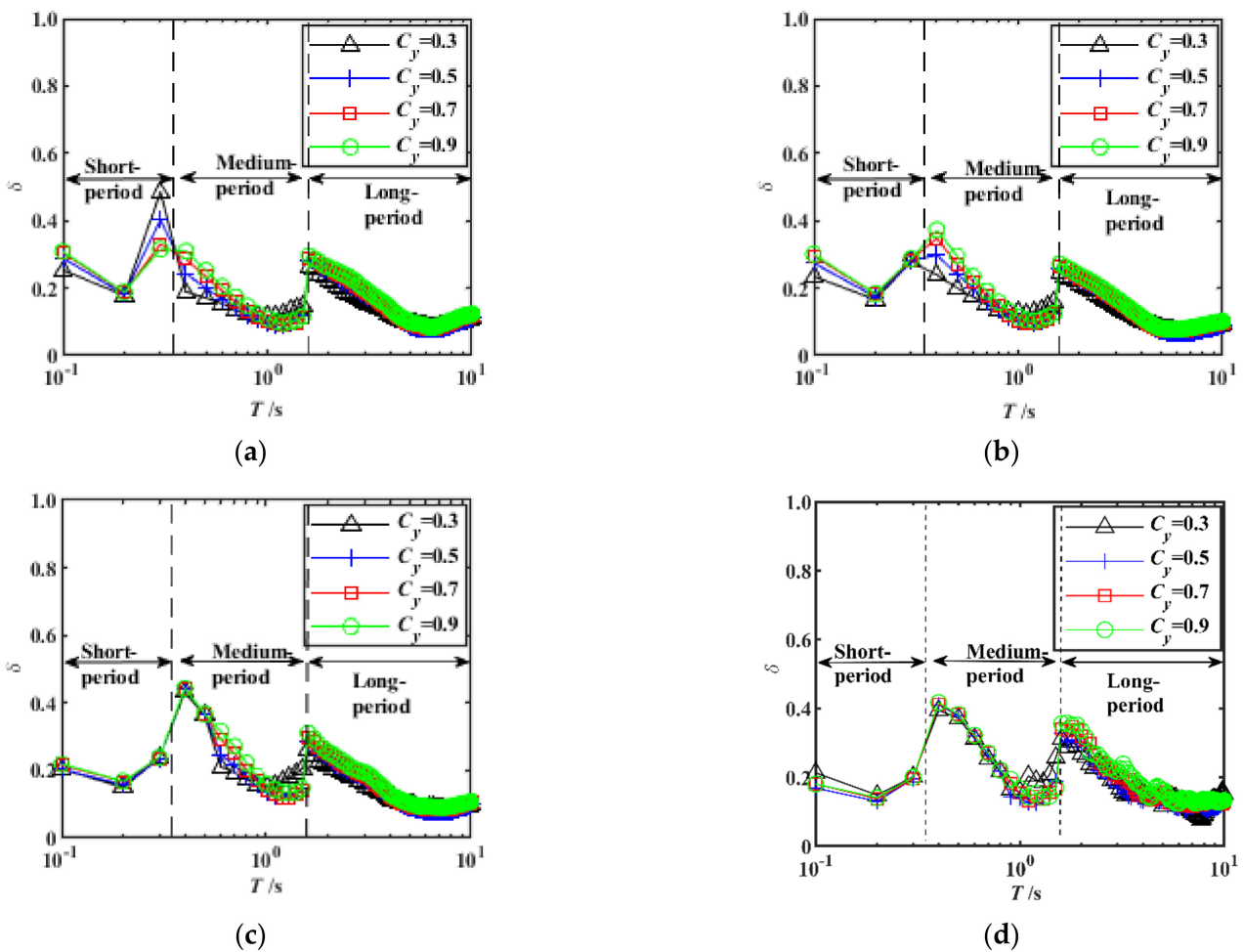


Figure 6. Cont.



**Figure 6.** The correlation results between the recommended damage potential ranking and the damage potential ranking under different  $C_y$  and  $T$  conditions on different sites: (a) type I site; (b) type II site; (c) type III site; (d) type IV site.



**Figure 7.** Discreteness results between the recommended damage potential ranking and the damage potential ranking under different  $C_y$  and  $T$  conditions on different sites: (a) type I site; (b) type II site; (c) type III site; (d) type IV site.

**Table 4.** Mean correlation coefficient and standard deviation between recommended damage potential ranking and damage potential ranking under different  $C_y$  and  $T$  conditions on different sites ( $p < 0.05$ ).

Site Factor	Short-Period Range		Medium-Period Range		Long-Period Range	
	$R$	$\delta$	$R$	$\delta$	$R$	$\delta$
Type I site	0.865	0.213	0.966	0.155	0.972	0.123
Type II site	0.906	0.243	0.955	0.160	0.978	0.115
Type III site	0.937	0.263	0.918	0.178	0.973	0.118
Type IV site	0.953	0.233	0.909	0.190	0.958	0.148
Not consider site factor	0.915	0.243	0.937	0.163	0.970	0.113

It is worth noting that the site factor is considered as a very important effect factor when selecting input ground motions for a seismic design [24,36]. The main reason for this is that the characteristics of ground motion are greatly affected by the site factor, and a resonance effect will occur when the natural vibration period of the structure is close to the characteristic period of ground motion. However, the structural response of the SDOF system is directly used as the damage potential  $IMs$  of ground motion in this paper, and the natural vibration period of the same type of structures are similar. If the resonance response occurs, the resonance response will be generated for all structures of the same types. Thus, the correlation and dispersion results are hardly affected by these types of sites.

## 6. Rationality Demonstration Based on MDOF Shear Structures

### 6.1. Structural Models

In this paper, the period range from 0 to 10 s is divided into a short-period range, a medium-period range, and a long-period range based on the improved Newmark–Hall spectrum. At the same time, the effects of  $C_y$ ,  $T$ , and the type of site on the damage potential  $IMs$  in each type of structure are analyzed, and some rules are obtained from the analysis results. However, are these variation laws also applicable to MDOF structures? This paper establishes two MDOF structural models for detailed demonstration based on the improved I–M–K model with reference to the relevant literature [37,38]. Additionally, the shear structural models of 8- and 12-story RC structures are established. The hysteretic skeleton line and structure model of the structure are shown in Figure 8. The relevant structure parameter settings are shown in Table 5. Additionally, in this table,  $T_1$  is the natural vibration period of the structure. It can be obtained that both structures belong to the medium-period structure:  $H_i$  is the height of each story of the structure, and  $W_i$  is the weight of each story of the structure.  $K_{ei}$  is the initial stiffness of each story of the structure.  $F_{yi}$  is the yield strength of each story of the structure,  $a_s$  is the stiffness ratio of the strengthening section of each story of the structure, and  $a_c$  is the stiffness ratio of the softening section of each story of the structure.

**Table 5.** Correlative structural parameters of improved I–M–K hysteretic model.

Structural Models	Story	$T_1$ (s)	$H_i$ (mm)	$W_i$ (kg)	$K_{ei}$ (kN·mm <sup>-1</sup> )	$F_{yi}$ (kN)	$a_s$	$a_c$	$u_c/u_y$	$\zeta$
8-story	1–8	0.82	3300	600	100	3000	0.05	−0.05	5	0.05
12-story	1–12	1.24	3300	600	100	3000	0.05	−0.05	5	0.05

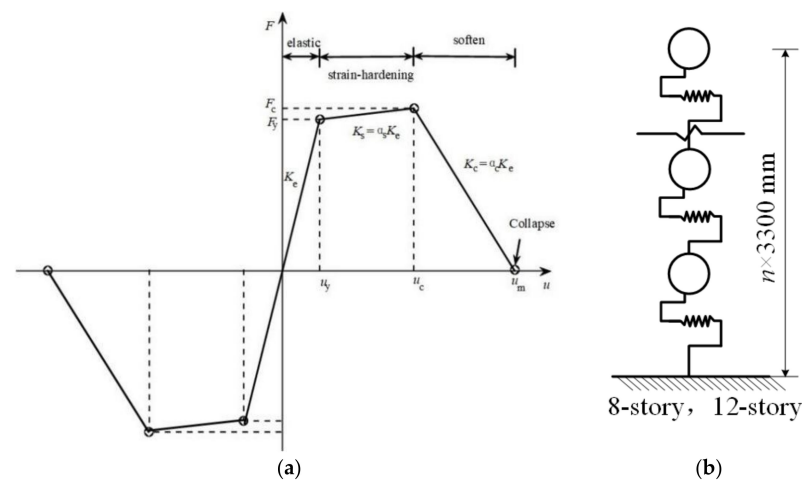


**Figure 8.** Hysteretic skeleton line and structural model of reinforced concrete shear structure: (a) hysteretic skeleton line; (b) structural model.

### 6.2. Rationality Demonstration

To demonstrate the effects of  $C_y$ ,  $T$ , and the type of site on the damage potential ranking, 5535 ground motion records were input into the 8-story and 12-story RC shear structures for nonlinear analysis. The correlation between the damage potential ranking and the structural response ranking was quantitatively evaluated by the  $R^2$ . The effects of  $C_y$  and  $T$  on the correlation results is shown in Figure 9. It can be obtained that, in the medium-period range, when the  $C_y$  is constant and the  $T$  changes, the  $R^2$  changes obviously, and the  $R^2$  is maximal at the natural vibration period  $T_1$  of the structure. When the  $C_y$  changes with the constant period, the  $R^2$  changes much less. Additionally,  $R^2$  ranges from 0.63 to 0.88, indicating a strong correlation between the damage potential ranking and the structural response ranking. It can also be seen in the results that the  $R^2$  between the damage potential ranking based on  $S_d(T_{ave}, C_{y,ave})$  and the structural response rankings of the 8-story and 12-story RC structures are both very high, with  $R^2$  values of 0.89 and 0.94, respectively. Therefore, it is reasonable to use  $S_d(T_{ave}, C_{y,ave})$  as the damage potential ranking of the medium-period structure. Figure 10 shows the correlation results of the damage potential ranking and structural response ranking based on ground motions in type I and III sites. For the specific structure, the  $R^2$  of the type I site is slightly higher than that of type III site. However, the  $R^2$  is above 0.8, and the correlation is very strong. Therefore, it can be concluded that, when ranking ground motions based on damage potential IMs, the effects of the site factor on damage potential ranking need not be considered.

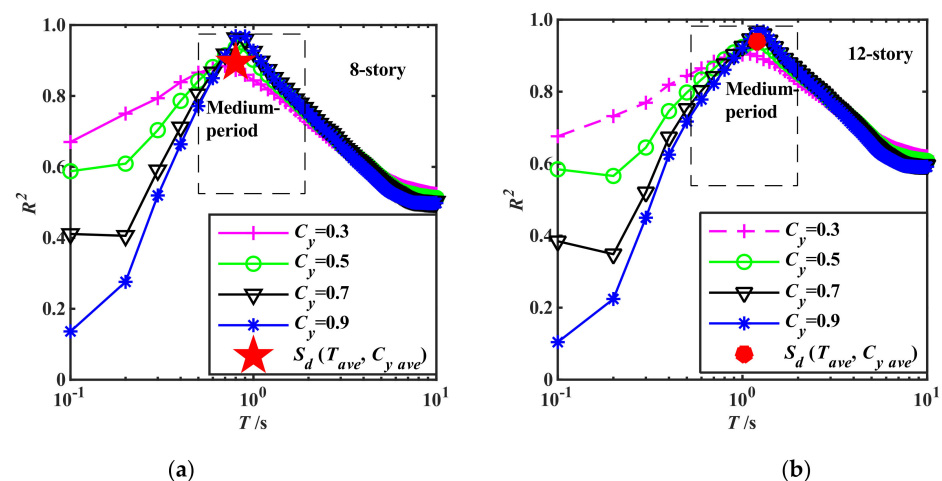


**Figure 9.** Correlation analysis of damage potential ranking and structural response corresponding to different  $T$  and  $C_y$ : (a) 8-story; (b) 12-story.

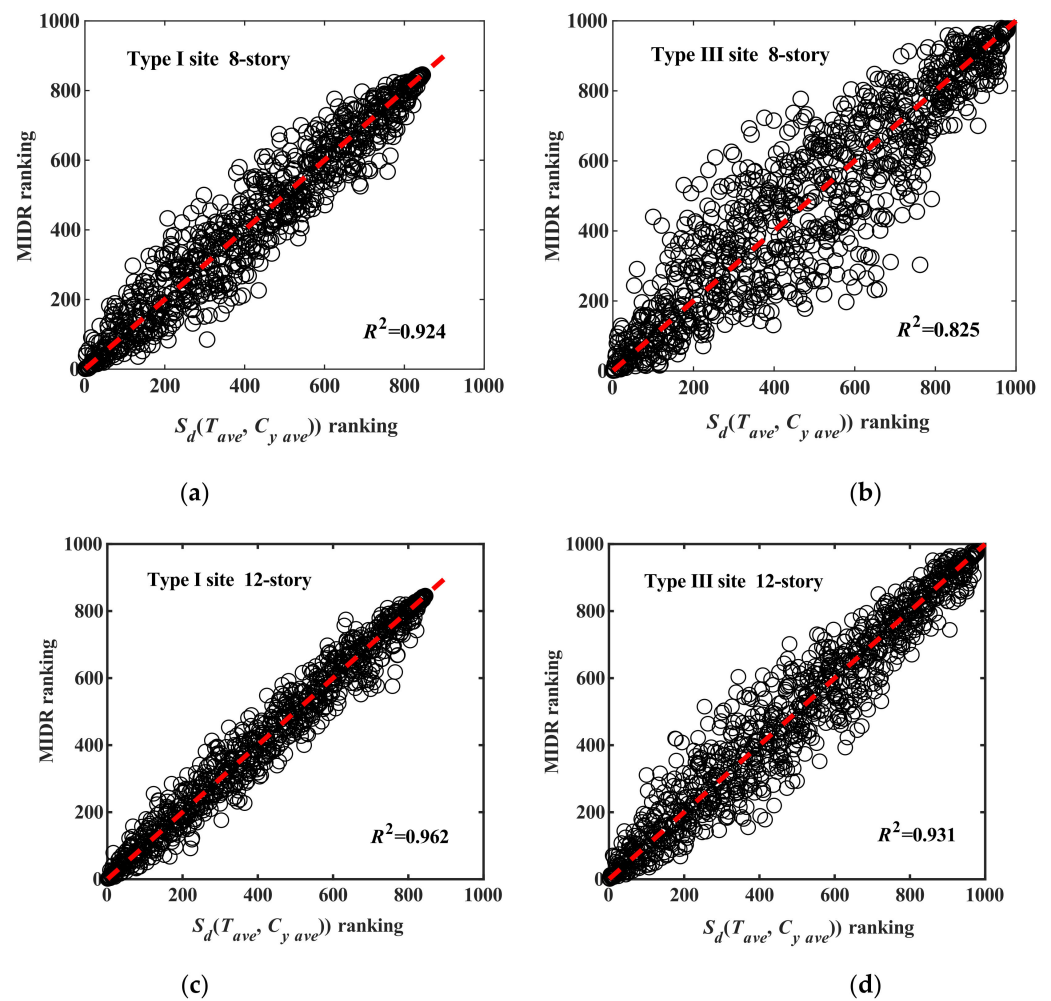


**Figure 10.** Correlation analysis between damage potential ranking and structural response ranking on different sites: (a) type I site (8–story); (b) type III site (8–story); (c) type I site (12–story); (d) type III site (12–story).

## 7. Conclusions

The structural period range was firstly divided based on the improved Newmark–Hall spectrum and 5535 horizontal ground motion records were used for the analysis. In structures of the same types, the correlation and discreteness analysis between the recommended damage potential ranking of ground motions and the damage potential ranking under different  $C_y$  and  $T$  conditions in the same period range were analyzed, and two shear structures were established to demonstrate the effect of the obtained variation law, and the following conclusions were obtained.

- (1) Based on the improved Newmark–Hall spectrum, the structure period range from 0 to 10 s is divided into three period ranges: short-period range ( $T < 0.40$  s), medium-period range ( $0.40 \text{ s} \leq T < 1.55$  s), and long-period range ( $T \geq 1.55$  s);
- (2) The recommended damage potential ranking and the damage potential ranking under different  $C_y$  and  $T$  conditions in the same period range has a large correlation, and the dispersion is small. The  $C_y$  and  $T$  have small effects on the damage potential ranking of ground motions in each period range, and the selected damage potential IMs are reasonable;
- (3) For the same types of structures, whether site factors are considered or not, the discreteness and correlation analysis between the recommended damage potential ranking of ground motions and the damage potential ranking under different  $C_y$  and

$T$  conditions are a little different. Therefore, it is unnecessary to consider the site factor when ranking the damage potential of ground motions;

- (4) Through the analysis of two shear structures, the  $R^2$  of the damage potential ranking and structure response ranking were found to be 0.89 and 0.94, respectively, which proves that the solution method of  $C_y$ ,  $T$ , and the type of site in this paper is reasonable when establishing damage potential ranking.

It is worth noting that the recommended damage potential ranking in the medium-period range has been demonstrated. It is also necessary to verify the recommended damage potential rankings in short- and long-period ranges based on representative MDOF structures in a further study.

**Author Contributions:** Conceptualization, Q.L. and J.H.; methodology, L.X. (Lili Xie); software, Q.L.; validation, Q.L., J.H., L.X. (Lili Xie) and L.X. (Longjun Xu); formal analysis, L.X. (Longjun Xu); investigation, Q.L.; resources, Q.L.; data curation, Q.L.; writing—original draft preparation, Q.L.; writing—review and editing, J.H.; visualization, J.H.; supervision, L.X. (Lili Xie); project administration, L.X. (Longjun Xu); funding acquisition, L.X. (Longjun Xu). All authors have read and agreed to the published version of the manuscript.

**Funding:** The work is supported by the National Natural Science Foundation of China (Grant No. U2139207; U1939210).

**Institutional Review Board Statement:** Not applicable.

**Informed Consent Statement:** Not applicable.

**Data Availability Statement:** Not applicable.

**Acknowledgments:** The work is supported by the National Natural Science Foundation of China (Grant No. U2139207; U1939210). The support is gratefully acknowledged. The authors would also like to thank the NGA-West2 database for providing the strong ground motion data.

**Conflicts of Interest:** The authors declare no conflict of interest.

## References

- Li, C.; Li, H.N.; Hao, H.; Bi, K.; Chen, B. Seismic fragility analyses of sea-crossing cable-stayed bridges subjected to multi-support ground motions on offshore sites. *Eng. Struct.* **2018**, *165*, 441–456. [[CrossRef](#)]
- Kostinakis, K.; Fontara, I.K.; Athanatopoulou, A.M. Scalar structure-specific ground motion intensity measures for assessing the seismic performance of structures: A review. *J. Earthq. Eng.* **2018**, *22*, 630–665. [[CrossRef](#)]
- Salami, M.R.; Kashani, M.M.; Goda, K. Influence of advanced structural modeling technique, mainshock-aftershock sequences, and ground-motion types on seismic fragility of low-rise RC structures. *Soil Dyn. Earthq. Eng.* **2019**, *117*, 263–279. [[CrossRef](#)]
- Tang, L.; Zhang, Y.; Ling, X.; Tian, S. Fuzzy optimization for ground motion intensity measures to characterize the response of the pile-supported wharf in liquefiable soils. *Ocean Eng.* **2022**, *265*, 112645. [[CrossRef](#)]
- Li, C.; Zhai, C.; Kunnath, S.; Ji, D. Methodology for selection of the most damaging ground motions for nuclear power plant structures. *Soil Dyn. Earthq. Eng.* **2019**, *116*, 345–357. [[CrossRef](#)]
- Marano, G.C.; Quaranta, G. A new possibilistic reliability index definition. *Acta Mech.* **2010**, *210*, 291–303. [[CrossRef](#)]
- Zhai, C.; Li, S.; Xie, L.; Sun, Y. Study on inelastic displacement ratio spectra for near-fault pulse-type ground motions. *Earthq. Eng. Eng. Vib.* **2007**, *6*, 351–355. [[CrossRef](#)]
- Xie, L.L.; Zhai, C.H. Study on the severest real ground motion for seismic design and analysis. *Acta Seismol. Sin.* **2003**, *16*, 260. [[CrossRef](#)]
- Yi, W.J.; Zhang, H.Y.; Kunnath, S.K. Probabilistic constant-strength ductility demand spectra. *J. Struct. Eng.* **2007**, *133*, 567–575. [[CrossRef](#)]
- Rosso, M.M.; Asso, R.; Aloisio, A.; Di Benedetto, M.; Cucuzza, R.; Greco, R. Corrosion effects on the capacity and ductility of concrete half-joint bridges. *Constr. Build. Mater.* **2022**, *360*, 129555. [[CrossRef](#)]
- Ji, D.; Wen, W.; Zhai, C. Constant-ductility energy factors of SDOF systems subjected to mainshock–aftershock sequences. *Earthq. Spectra* **2021**, *37*, 1078–1107. [[CrossRef](#)]
- Hu, J.J.; Lai, Q.H.; Liu, X.; Xie, L. Effects of structural and seismic factors on the constant-strength ductility spectra based on NGA-West2 database. *Shock Vib.* **2020**, *4*, 8820582. [[CrossRef](#)]
- Aloisio, A.; Rosso, M.M.; Iqbal, A.; Fragiaco, M. Hysteresis modeling of timber-based structural systems using a combined data and model-driven approach. *Comput. Struct.* **2022**, *269*, 106830. [[CrossRef](#)]
- Fiore, A.; Marano, G.C.; Monaco, P. Earthquake-induced lateral-torsional pounding between two equal height multi-storey buildings under multiple bi-directional ground motions. *Adv. Struct. Eng.* **2013**, *16*, 845–865. [[CrossRef](#)]

15. Ning, C.L.; Wang, S.; Cheng, Y. An explicit solution for the effect of earthquake incidence angles on seismic ductility demand of structures using Bouc-Wen model. *Soil Dyna. Earthq. Eng.* **2022**, *153*, 107085. [[CrossRef](#)]
16. Lu, X.L.; Zhou, D.S. Ductility demand spectra and inelastic displacement spectra considering soil conditions and design characteristic periods. *Earthq. Eng. Eng. Vib.* **2004**, *24*, 39–48. (In Chinese)
17. Rupakhety, R.; Sigbjornsson, R. Ground-motion prediction equations (GMPEs) for inelastic displacement and ductility demands of constant-strength SDOF systems. *Bull. Earthq. Eng.* **2009**, *7*, 661–679. [[CrossRef](#)]
18. Miranda, E.; Bertero, V.V. Evaluation of strength reduction factors for earthquake resistant design. *Earthq. Spectra* **1994**, *10*, 357–379. [[CrossRef](#)]
19. Miranda, E. Inelastic Displacement ratios for structures on firm sites. *J. Struct. Eng.* **2000**, *126*, 1150–1159. [[CrossRef](#)]
20. Baker, J.W.; Cornell, C.A. A vector-valued ground motion intensity measure consisting of spectral acceleration and epsilon. *Earthq. Eng. Struct. Dyn.* **2005**, *34*, 1193–1217. [[CrossRef](#)]
21. Baker, J.W.; Cornell, C.A. Spectral shape, epsilon and record selection. *Earthq. Eng. Struct. Dyn.* **2006**, *35*, 1077–1095. [[CrossRef](#)]
22. Baker, J.W. Efficient analytical fragility function fitting using dynamic structural analysis. *Earthq. Spectra* **2015**, *31*, 579–599. [[CrossRef](#)]
23. Baker, J.W. Conditional mean spectrum: Tool for ground-motion selection. *J. Struct. Eng.* **2011**, *137*, 322–331. [[CrossRef](#)]
24. *GB 50011-2010*; Code for Seismic Design of Buildings. China Architecture & Building Press: Beijing, China, 2010.
25. Guo, F.; Wu, D.M.; Xu, G.F.; Ji, Y.L. Site classification corresponding relationship between Chinese and the overseas seismic design codes. *J. Civ. Eng. Manag.* **2011**, *28*, 63–66. (In Chinese) [[CrossRef](#)]
26. Hu, J.J.; Lai, Q.H.; Li, S.; Xie, L.L. Procedure for ranking ground motion records based on the destructive capacity parameter. *KSCE J. Civ. Eng.* **2020**, *25*, 197–207. [[CrossRef](#)]
27. Newmark, N.M.; Blume, J.A.; Kapur, K.K. Seismic Design Spectra for Nuclear Power Plants. *ASCE Power Div. J.* **1973**, *99*, 287–303. [[CrossRef](#)]
28. Seed, H.B.; Ugas, C.; Lysmer, J. Site-dependent spectra for earthquake-resistant design. *Bull. Seismol. Soc. Am.* **1976**, *66*, 221–243. [[CrossRef](#)]
29. Xu, L.J.; Zhao, G.C.; Liu, Q. Consecutive combined response spectrum. *Earthq. Eng. Eng. Vib.* **2014**, *13*, 623–636. [[CrossRef](#)]
30. Xiong, C.; Lu, X.; Lin, X.; Xu, Z.; Ye, L. Parameter determination and damage assessment for THA-based regional seismic damage prediction of multi-story buildings. *J. Earthq. Eng.* **2017**, *21*, 461–485. [[CrossRef](#)]
31. Jalayer, F.; Beck, J.L.; Zareian, F. Analyzing the Sufficiency of Alternative Scalar and Vector Intensity Measures of Ground Shaking Based on Information Theory. *J. Eng. Mech.* **2012**, *138*, 307–316. [[CrossRef](#)]
32. Mahaney, J.A.; Paret, T.F.; Kehoe, B.E.; Freeman, S.A. The capacity spectrum method for evaluating structural response during the Loma Prieta earthquake. In *Mitigation and Damage to the Built Environment*; U.S. Central United States Earthquake Consortium (CUSEC): Memphis, TN, USA, 1993.
33. Zhang, R.; Wang, D.S.; Chen, X.Y.; Li, H.N. Weighted scaling and selecting method of ground motions in time-history analysis considering influence of higher modes. *China Civ. Eng. J.* **2019**, *52*, 53–68. (In Chinese) [[CrossRef](#)]
34. Yakhchalian, M.; Amiri, G.G. A vector intensity measure to reliably predict maximum drift in low- to mid-rise buildings. *Struct. Build.* **2018**, *172*, 42–54. [[CrossRef](#)]
35. Wang, D.H. *Multivariate Statistical Analysis and SPSS Application*; East China University of Science and Technology Press: Sanghai, China, 2010. (In Chinese)
36. *ASCE/SEI 7-16*; Minimum Design Loads for Buildings and Other Structures. American Society of Civil Engineers: Reston, VA, USA, 2016.
37. Ibarra, L.F.; Medina, R.A.; Krawinkler, H. Hysteretic models that incorporate strength and stiffness deterioration. *Earthq. Eng. Struct. Dyn.* **2005**, *34*, 1489–1511. [[CrossRef](#)]
38. Ibarra, L.F.; Krawinkler, H. Variance of collapse capacity of SDOF systems under earthquake excitations. *Earthq. Eng. Struct. Dyn.* **2011**, *40*, 1299–1314. [[CrossRef](#)]

**Disclaimer/Publisher's Note:** The statements, opinions and data contained in all publications are solely those of the individual author(s) and contributor(s) and not of MDPI and/or the editor(s). MDPI and/or the editor(s) disclaim responsibility for any injury to people or property resulting from any ideas, methods, instructions or products referred to in the content.